[TITLE]

Apatite-coated hyaluronan for bone regeneration

[ARTICLE TYPE]

Research report (Biomaterials & Bioengineering)

[AUTHORS]

K. Tanaka[1], T. Goto[2*], T. Miyazaki[3], Y. Morita[3], S. Kobayashi[2], and T. Takahashi[1]

[1]Division of Oral and Maxillofacial Reconstructive Surgery, and [2] Division of Anatomy, Kyushu Dental College, Kitakyushu, 803-8580 Japan.

[3]Graduate School of Life Science and Systems Engineering, Kyushu Institute of Technology, Kitakyushu, 808-0196, Japan; *corresponding author.

[CORRESPONDING AUTHOR]

Tetsuya Goto, D.D.S., PhD

Division of Anatomy, Kyushu Dental College,

2-6-1 Manazuru, Kokurakita-ku, Kitakyushu, 803-8580, Japan

Tel: +81-93-285-3030

Fax: +81-93-591-8199

E-mail: tgoto@kyu-dent.ac.jp

[RUNNING TITLE]

Apatite-coated hyaluronan

[KEY WORDS]

Hyaluronan

Apatite

Osteoblast

Bone regeneration

[NUMBER OF WORDS]

Abstract: 182 words

Abstract and text: 2,498 words

[NUMBER OF TABLES AND FIGURES]

4

[NUMBER OF CITED REFERENCES]

24

ABSTRACT

The materials for the bone defects require bone inductive and bioabsorbable properties. We developed an apatite-coated hyaluronan (ACH) for the material of bone regeneration. To examine its biocompatibility and bone-inductive activity, we evaluated the proliferation and differentiation of osteoblast-like cells grown on ACH *in vitro,* and examined the effect of ACH on bone regeneration *in vivo*, comparing these with atelocollagen sponge (AS). Hyaluronic acid, cross-linked by divinylsulfone, was freeze-dried and formed apatite in simulated body fluid. MC3T3-E1 osteoblast-like cells were cultured on ACH and AS. Alkaline phosphates activity and osteocalcin mRNA expression increased more in cells grown on ACH than in those grown on AS. *In vivo*, round defects were created in rat crania and filled in with ACH, AS, or nothing (sham group). After surgery, the ACH-treated group showed higher levels of bone formation than the other groups. These findings demonstrate that ACH is a more effective than AS in promoting *in vitro* osteoblast-like cell differentiation and bone formation during the repair of bone defects *in vivo*, indicating that it may be of use in the treatment of various bone defects.

INTRODUCTION

Inducing bone augmentation while minimizing procedural invasiveness is a great challenge not only in implant dentistry but also for the future of clinical medicine. Autologous bone grafting is widely used to increase bone volume. However, only small amounts of donor bone may be safely used, and bone resorption following surgery is unpredictable (Hoppenreijs *et al*., 1992). An alternative method for augmenting skeletal structures involves the use of various xenogenic materials, including types of apatite (LeGeros, 2002). Since apatite materials offer osteoconductivity, which allows bone cells to grow on their surface, apatite materials have been used in clinical practice (Ozawa and Kasugai, 1996; Anselme, 2000; Okumura *et al.,* 2001; Sibilla *et al.*, 2006). However, these materials have lower fracture toughness than cortical bone has, their use as bone substitutes in load-bearing parts of the human skeleton has been problematic.

In one approach for generating apatite–polymer hybrids, the apatite is deposited in simulated body fluid (SBF) or a related solution on a substrate abundant in functional groups. An apatite–polymer hybrid is prepared through the spontaneous deposition of apatite crystals on an organic polymer in a body environment if the surface of the polymer contains many carboxyl groups (-COOH) and Ca^{2+} ions (Miyazaki *et al.*, 2003).

Hyaluronic acid, hyaluronan, is one of the major components of the extracellular matrix (ECM), and has an abundance of carboxyl groups. By binding to cellular receptors, hyaluronan

regulates various biological processes including osteoconduction, wound repair, inflammation, and metastasis (Pilloni and Bernard, 1998; Zou *et al*., 2008). Furthermore, our recent study could induce the deposition of apatite into porous hyaluronic acid abundant in carboxyl groups using SBF, and thereby produced apatite-coated hyalunoran (ACH) (Morita *et al*., 2009).

The aims of this study were to investigate adhesion, spreading, and expression of osteogenic genes in MC3T3-EI osteoblastic cells cultured on ACH or on atelocollagen sponge (AS) that is clinically used in bone repair. Furthermore, we examined the effects of apatite-coated hyaluronan on bone regeneration during the repair of rat cranial defects.

MATERIALS & METHODS

Preparation of apatite-coated hyaluronan

As we described previously (Morita *et al.*, 2009), a powder preparation of hyaluronic acid ($C_{14}H_{20}NNaO_{11}$; Nacalai Tesque, Kyoto, Japan) was dissolved in 0.01 NaOH at a concentration of 1% w/v. Then, the cross-linking agent divinylsulfone (DVS) ($(H_2SCH)_2SO_2$; Wako Pure Chemical Industries, Ltd. Osaka, Japan) (0.5% w/v) was added. The resulting solution was poured into a polystyrene container and dried in a vacuum freeze drier at -80°C. The samples were then soaked in a 1M $CaC1_2$ at 36.5°C for 24h, and subsequently in SBF at 36.5°C for 7 days.

Surface analysis

The surface structure of ACH was examined using a scanning electron microscope (SEM) (Model S-3000N; Hitachi, Tokyo, Japan), an energy dispersal X-ray (EDX) spectrophotometer (Model 7021-H; Horiba, Kyoto, Japan), and a thin-film radiographic diffractometer (TF-XRD) (Model M03XHF2 2; MAC Science, Kanagawa, Japan). For the TF-XRD analysis, the angle of the incident beam was fixed at 1 degree to the surface of the sample.

Cell culture

ACH was sterilized by autoclaving and applied to 48-well dish plates or 35-mm dishes. Additional plates were lined with AS (Terudermis^{TM}, Olympus Terumo Biomaterials Corp., Tokyo, Japan), an absorbable atelocollagen cross-linked by heat treatment. Mouse osteoblastic MC3T3-E1 cells were seeded onto ACH and AS at concentrations of 1×10^3 or 5×10^4 cells per dish, respectively. Cells were grown in α-Minimum Essential Medium (αMEM) (Gibco, Grand Island, NY, USA) supplemented with 10% fetal bovine serum (Wako), for 24 h, and thereafter in osteogenic medium (αMEM with 10 nM β-glycerol phosphate (SIGMA, St Louis, MO, USA), 10 nM β-ascorbic acid (Wako)). Cells were harvested after 4, 7, and 14 days.

Actin staining

To determine the number and the area of cells, actin staining was performed. After 24 or 48 h culture, cells were washed with cytoskeleton-stabilizing (CS) buffer and fixed in 4% formalin. After 3 additional washes in CS buffer, they were next incubated for 30 min at 37°C with tetramethylrhodamine isothiocyanate (TRITC)-phalloidin (diluted 1:40) (Molecular Probes,

Eugene, OR, USA).

Alkaline Phosphatase Activity Assay

Four or 7 days after cell seeding, the cells were then homogenized for 2 min and centrifuged at 2,000 rpm for 10 min. Supernatant alkaline phosphatase (ALP) activity was measured using an ALP Activity Assay Kit (Wako) according to the manufacturer's instructions.

Semi-quantitative RT-PCR

Fourteen days after seeding, cellular mRNA was extracted using a Total RNA Extraction Miniprep System (Viogene, Sunnyvale, CA, USA) in accordance with the manufacturer's protocol. cDNA was synthesized from total RNA (2 μg) in reaction buffer (30 μl) composed of dNTPs (500 μM), ribonuclease inhibitor (20 U) (Promega, Madison, WI, USA), and Superscript II reverse transcriptase (200 U) (Invitrogen Life Technologies, Carlsbad, CA, USA). Oligonucleotide primers were designed for use in reverse transcriptase-PCR (RT-PCR). The primers used in this study are listed in Appendix 1.

Surgical procedures

All experiments followed the guidelines of the Animal Use and Care Committee of Kyushu Dental College. Thirty-six male Wister rats weighing 300–350 g were used. Animals were anesthetized through intramuscular injections of xylazine (13 mg/kg) (Bayer, Tokyo, Japan). A midline incision was made down to the depth of the surface of the skull, and a skin–periosteal flap was raised to expose the bone on both sides of the midline. Under generous irrigation with

saline, cranial bone was removed by trephine bur. Six mm-diameter cranial bone defects were created in both sides of the skull (one per side). The holes were filled in with ACH, AS, or nothing (sham group).

Specimen preparation and analysis

One and 3 weeks after surgery, under deep anesthesia, rats were perfused transcardially with 4% paraformaldehyde in 0.1 M PBS. The crania were removed and decalcified in 10% EDTA for 2 weeks. After decalcification, the bone tissue was frozen and cut into 8-μm-thick sections using a cryostat (Leica Instruments, Tokyo, Japan). Bone sections were stained with 1% toluidine blue or subjected to immunohistochemical analysis. In the latter case, sections were incubated for 10 min in 0.1 M PBS containing 0.3% H_2O_2, rinsed with PBS, and incubated for 30 min at room temperature in 0.1 M PBS containing 1% normal goat serum (Cosmo Bio Co., Ltd, Tokyo, Japan). They were then incubated for 2 hours at room temperature with a mouse polyclonal antibody against osteopontin (diluted 1:80) (Cosmo Bio). After rinsing with PBS, the sections were incubated with avidin–biotin–peroxidase complex from a VECTASTAIN Elite ABC KIT (Vector Laboratories, Burlingame, CA, USA). Peroxidase activity was detected using 0.02% 3,3'-diaminobenzidine (Dojindo, Kumamoto, Japan) and a 0.02% solution of hydrogen peroxidase. Morphometric measurements were taken from histological sections prepared from specimens of calcified bone using a microscope (Handy Scope 130s, Science-Eye, Saitama, Japan).

Statistical Analysis

The data were analyzed using StatView software (Abacus Concepts, Berkeley, CA, USA). One-way analysis of variance (ANOVA) was used to evaluate the effects of ACH and AS. Post-hoc comparisons were made using the Scheffé test.

RESULTS

Using our methods, we obtained various sizes of ACH with soft surfaces that we could easily bend (Fig. 1A, B).

SEM analysis of apatite-coated hyaluronan revealed rough surfaces showing deposition of domed apatite-like particles (Fig. 1C). EDX analysis of these deposits, formed on the freeze-dried hyaluronic acid gels, confirmed that they included minerals of calcium and phosphorus (Fig. 1D). The TF-XRD spectra produced by ACH included broad peaks (with 2 θ values of 26°and 32°), which were attributed to hydroxyapatite of low crystallinity (Fig. 1E). These findings suggest that the deposits on the freeze-dried hyaluronic acid gels were composed of low-crystalline apatite.

The cells on ACH and AS were visualized by actin staining (Fig. 2A-D). At 24 and 48 h, significantly fewer cells were attached to ACH than to AS (Fig. 2E). At 24 h, the mean spreading area of cells grown on ACH was higher than that of cells grown on AS (although not to a statistically significant extent). However, at 48 h the mean spreading area of cells grown on ACH

was significantly lower than that of cells grown on AS (Fig. 2F).

ALP is a marker of the early stages of osteoblast differentiation. ALP activity, assessed 4 and 7 days after cells were seeded onto ACH and AS, was significantly higher in cells grown on ACH than in cells grown on AS (Fig. 3A).

Semi-quantitative RT-PCR was performed to analyze the expression of the osteoblastic differentiation markers runx-2, osterix, type I collagen (Col I), and osteocalcin (OCN) in osteoblastic cells grown on ACH and AS (Fig. 3B). Runx-2, osterix, and Col 1 were expressed at similar levels in cells grown on ACH and AS. Expression of OCN, a marker of late-stage osteoblast differentiation, was higher in cells grown on ACH than in those seeded onto AS.

Bone defects created in rat calvariae were filled with ACH and AS to assess their relative effects on *in vivo* bone regeneration. At one week after surgery, the defects had not been repaired in animals treated with ACH or AS or sham controls (Fig. 4A, C, E). By 3 weeks post-surgery, only a small amount of bone had been regenerated in animals in the sham group (Fig.4B). This newly formed bone was localized at the boundary of the defect, and the holes were mostly filled with soft tissue. In bone defects filled with ACH or AS, new bone had formed (Fig. 4D, F). ACH and AS themselves were scarcely detected. The area of new bone in ACH group (1.49 ± 0.30 mm^2) exceeded that in AS (0.99 ± 0.13 mm^2) and sham groups (0.73 ± 0.16 mm^2) (Fig. 4G). Three weeks after surgery, the cells surrounding newly formed bone in animals treated with ACH were osteopontin immunopositive, indicating that they were osteoblasts (Fig. 7H, I).

DISCUSSION

In this study, we demonstrated the ability of ACH to stimulate bone-forming activities *in vitro* and *in vivo*. This hybrid compound has a soft surface and high flexibility, which suggests that it may be useful in treating bone defects of various shapes.

In this study, freeze-dried hyaluronan soaked in SBF accumulated apatite deposits on their surfaces, as identified by SEM and surface analyses. Boskey and Dick (1991) reported that hyaluronic acid stimulates the growth and proliferation of hydroxyapatite crystals in a concentration-dependent fashion. Elsewhere, it was shown that $CaC1_2$ enhances the formation of apatite deposits on polyglutamic acid hydrogels soaked in SBF (Sugino *et al.*, 2008). COOH groups, abundant in the polyglutamic acid hydrogels, act as heterogeneous nucleation sites for apatite crystal formation. It is known that sulfonyl groups can nucleate apatite crystallization *in vivo* (Kawai *et al*., 2004). Therefore, the sulfonyl group of DVS may also play a role in apatite nucleation, giving rise to fine apatite particles. Its thin apatite coating confers freeze-dried hyaluronan with a suitable hardness for clinical use, as well as osteoconductive activity.

Several researchers have reported that cell motility/morphogenesis is strongly dependent on the surface topography or surface chemistry of the materials to which cells adhere (El-Ghannam *et al.*, 1997; Ducheyne and Qiu; 1999). MC3T3-E1 cells showed less attachment on ACH and spread than AS did, which means collagen is better substrate for the attachment of osteoblastic cells. Furthermore, the mean area of ACH covered by adherent cells increased less in a 24-hr

period than AS. These results are consistent with our previous finding that osteoblastic cells seeded to hydroxyapatite spread less than did those seeded to titanium. The cells on the apatite spread and became stable, which may have induced them to start matrix production. (Okumura *et al*., 2001).

The effects of hydroxyapatite on ALP activity and osteogenic gene expression in osteoblast-like cells support previous reports that biomaterials enhance cell functions that favor osteoblastic cell differentiation (Hong *et al.*, 2003; Sibilla *et al.*, 2006). The high level of ALP activity in cells grown on hydroxyapatite was reported to promote the formation of mineralized tissue (Ozawa and Kasugai, 1996). In the present study, we found significantly high ALP activity in the cells grown on ACH compared with cells grown on AS. These results suggest that ACH possesses the ability to induce osteoblastic cell differentiation. Previous studies have examined the effects of hyaluronic acid on *in vitro* responses/parameters associated with osteogenesis (Pilloni and Bernard, 1998; Huang *et al.*, 2003). We additionally detected, by semi-quantitative RT-PCR, an increase in OCN mRNA expression. The osteoconductive properties of hydroxyapatite and hyaluronic acid suggest that ACH promotes *in vitro* differentiation of osteoblast-like cells more strongly than does AS.

Histomorphometry has been a useful tool in characterizing the extent of bone integration (Lin *et al*., 2007). ACH-treated rats showed bone formation at 3 weeks post-surgery and produced greater amounts of calvarial osteoid tissue than did animals in the other two test groups. Previous

in vivo studies reported the presence of osteoblasts on hydroxyapatite (Doyle *et al.*, 1991; Patel *et al.*, 2002; Chu *et al*., 2002). These findings illustrate the high biocompatibility and osteoinductivity of hydroxyapatite. Hyaluronic acid additionally enhances bone formation. First, hyaluronic acid effectively retains osteoinductive growth factors, and it is capable of accelerating new bone formation during bone wound healing by stimulating osteogenic cell differentiation *in vivo* (Pilloni and Bernard, 1998). Second, previous findings suggest that low molecular weight hyaluronic acid stimulates osteoclast differentiation (Ariyoshi *et al.*, 2005). Third, hyaluronic acid was found to stimulate bone resorption, which suggests that it may enhance bone remodeling (Prince, 2004). From our histomorphometric analyses, ACH exhibited potent osteoinductive properties that may be attributed to their constituents, hydroxyapatite and hyaluronic acid.

In summary, we found ACH promoted osteoblast-like cell differentiation *in vitro* and bone formation during the repair of bone defects *in vivo*, indicating that it may be of use in the treatment of various bone defects. Since ACH is highly flexible and can be applied to bone defects of various sizes, it is expected to be of use for promoting regeneration during the repair of bone defects.

ACKNOWLEGEMENTA

Support for this research was provided the grant form Kyushu Dental College to Tetsuya Goto.

REFERENCES

Anselme K (2000). Osteoblast adhesion on biomaterials. *Biomaterials* 21: 667-681 .

Ariyoshi W, Takahashi T, Kanno T, Ichimiya H, Takano H, Koseki T, Nishihara T (2005). Mechanisms Involved in Enhancement of Osteoclast Formation and Function by Low Molecular Weight Hyaluronic Acid. *J Biol Chem* 280; 18967-18972.

Boskey AL, Dick BL (1991). Hyaluronan interaction with hydroxyapatite do not alter in vitro hydroxyapatite crystal proliferation and growth. *Matrix* 11:442-446.

Chu TM, Orton DG, Hollister SJ, Feinberg SE, Halloran JW (2002). Mechanical and in vivo performance of hydroxyapatite implants with controlled architectures. *Biomaterials* 23; 1283–1293.

Doyle C, Tanner ET, Bonfield W (1991). In vitro and in vivo evaluation of polyhydroxybutyrate and of polyhydroxybutyrate reinforced with hydroxyapatite. *Biomaterials* 12; 841- 847.

Ducheyne P, Qiu Q (1999). Bioactive ceramics: the effect of surface reactivity on bone formation and bone cell function. *Biomaterials* 20; 2287-303.

El-Ghannam A, Ducheyne P, Shapiro IM (1997). Porous bioactive glass and hydroxyapatite ceramic affect bone cell function *in vitro* along different time lines. *J Biomed Mater Res* 36: 167–180.

Huang L, Cheng YY, Koo PL, Lee KM, Qin L, Cheng JC, Kumta SM (2003). The effect of hyaluronan on osteoblast proliferation and differentiation in rat calvarial-derived cell cultures. *J Biomed Mater Res* 66: 880–884.

Hong JY, Kim YJ, Lee HW, Lee WK, Ko JS, Kim HM (2003). Osteoblastic cell response to thin film of poorly crystalline calcium phosphate apatite formed at low temperatures. *Biomaterials* 24: 2977– 2984.

Hoppenreijs TJM, Nijdam ES, Freihofer HPM (1992). The chin as a donor site in early secondary osteoplasty: a retrospective clinical and radiological evaluation. *J Cranio-Maxillo-Facial Surg* 20: 119-124.

Kawai T, Ohtsuki C, Kamitakahara M, Miyazaki T, Tanihara M, Sakaguchi Y, Konagaya S (2004). Coating of an apatite layer on polyamide films containing sulfonic groups by a biomimetic process. *Biomaterials* 25:4529–4534.

LeGeros RZ (2002). Properties of osteoconductive biomaterials: calcium phosphates. *Clin Orthop Relat Res* 395: 81-98.

Lin Y, Wang T, Wu L, Jing W, Chen X, Li Z, Liu L, Tang W, Zheng X, Tian W (2007). Ectopic and in situ bone formation of adipose tissue-derived stromal cells in biphasic calcium phosphate nanocomposite. *J Biomed Mater Res A* 81; 900-910.

Miyazaki T, Ohtsuki C, Akioka Y, Tanihara M, Nakao J, Sakaguchi Y, Konagaya S (2003). Apatite deposition on polyamide films containing carboxyl group in a biomimetic solution. *J Mater Sci: Mater Med* 14: 569-574.

Morita Y, Matumoto C, Miyazaki T, Ishida E, Tanaka K, Goto T (2009). Apatite deposition on hyaluronic acid gels in biomimetic conditions. *Transaction MRS Japan* 34:85-87.

Okumura A, Goto M, Goto T, Yoshinari M, Masuko S, Katsuki T, Tanaka T (2001). Substrate affects the initial attachment and subsequent behavior of human osteoblastic cells (Saos-2). *Biomaterials* 22: 2263-2271.

Ozawa S, Kasugai S (1996). Evaluation of implant materials (hydroxyapatite, gass-ceramics, titanium) in rat bone marrow stromal cell culture. *Biomaterials* 17: 23-29.

Patel N, Best SM, Bonfield W, Gibson IR, Hing KA, Damien E, Revell PA (2002). A comparative study on the in vivo behavior of hydroxyapatite and silicon substituted hydroxyapatite granules. *J Mater Sci Mater Med* 13;1199-1206.

Pilloni A, Bernard GW (1998). The effect of hyaluronan on mouse intramembranous osteogenesis in vitro. *Cell Tissue Res* 294: 323–333.

Prince CW (2004). Roles of hyaluronan in bone resorption. *BMC Musculoskelet Disord* 29; 5-12.

Sibilla P, Sereni A, Aguiari G, Banzi M, Manzati E, Mischiati C, Sibilla P, Trombelli L, del Senno L (2006). Effects of a Hydroxyapatite-based Biomaterial on Gene Expression in Osteoblast-like Cells. *J Dent Res* 85; 354-358.

Sugino A, Miyazaki T, Ohtsuki C (2008). Apatite-forming ability of polyglutamic acid hydrogels in a body-simulating environment. *J Mater Sci: Mater Med* 19:2269–2274.

Zou X, Li H, Chen L, Baatrup A, Bünger C, Lind M (2004). Stimulation of porcine bone marrow stromal cells by hyaluronan, dexamethasone and rhBMP-2. *Biomaterials* 25: 5375–5385.

Zou L, Zou X, Chen L, Li H, Mygind T, Kassem M, Bünger C (2008). The effect of hyaluronan on osteogenic differentiation of porcine bone marrow stromal cells in vitro. *J Orthop Res* 26:713-720.

Legends

Figure 1. Apatite-coated hyaluronan (ACH) and its surface texture and property. **(A)** Overhead view of large-size ACH. Demonstration of ACH flexibility **(B)**. SEM images **(C)**, EDX data **(D)**, and TF-XRD patterns **(E)** of the surface of ACH, which were formed through cross-linking with divinylsulfone, freeze-dried, washed with 1M $CaCl_2$ for 24 h , and finally soaked in SBF for 7 days. Bar = 1.0 cm (A, B), 5 μm (C).

Figure 2. Attachment and spreading of osteoblastic cells cultured on ACH and atelocollagen sponge (AS). Fluorescent images showing actin fibers in osteoblastic cells cultured on apatite coated hyaluronan and atelocollagen sponge for 24 h and 48 h **(A–D)**. Number **(E)** and mean area **(F)** of cells adhered to ACH and AS. Cells in 10 randomly selected fields (50 x 70 μm) were examined using a fluorescence microscope (Olympus Optical, Tokyo, Japan). Data represent mean ± SD. * $p < 0.05$, ** $p < 0.01$. Bar = 10 μm (A-D).

Figure 3. Alkaline phosphate activity and gene expression of the MC3T3-E1 cells on ACH and AS. **(A)** ALP activity of the 4 or 7days cultured MC3T3-E1 cells was monitored spectrophotometrically using a microplate reader (Model 55C; Bio-Rad, Tokyo, Japan). Sample protein concentrations were measured using a commercially available kit (Protein Assay Rapid

Kit; Wako). Bovine serum albumin was used as a standard. Data represent mean ± SD. $^{**}p < 0.01$. **(B)** Semi-quantitative RT-PCR analysis of the gene expression in the MC3T3-E1 cells on ACH and AS cultured for 14 days. Osteoblast differentiation markers, runx-2, osterix, type I collagen (Col I), and osteocalcin (OCN) were detected in cells grown on ACH and AS. Reproducibility of the RT-PCR data was confirmed by three or more replicate experiments. Data were analyzed using NIH Image software (NIH, Bethesda, MD, USA). Values represent levels of target mRNA expression, quantified relative to loading control (β-actin) signals. MW: molecular weight markers.

Figure 4. Bone regenerative properties of apatite-coated hyaluronan. Histological images show bone formation in sham **(A, B)**, AS **(C, D)**, and ACH-treated rats **(E, F)**, 1 and 3 weeks after cranial bone defects were filled. CB: cranial bone. Vertical bars indicate the margins of the created bone defects. Arrows indicate newly formed bone. **(G)** Quantified areas of newly formed bone. Data represent means ± SD. $^{*}p < 0.05$. **(H)** Immunohistochemical detection of osteopontin (OPN) on the apatite-coated hyaluronan group 3 weeks after surgery. **(I)** Higher magnification image of the highlighted region in (H). Arrows identify a layer of OPN-positive cells. All slides were counterstained with toluidine blue. Bar = 1 mm (A-F), 0.5 mm (H), and 0.1 mm (I).

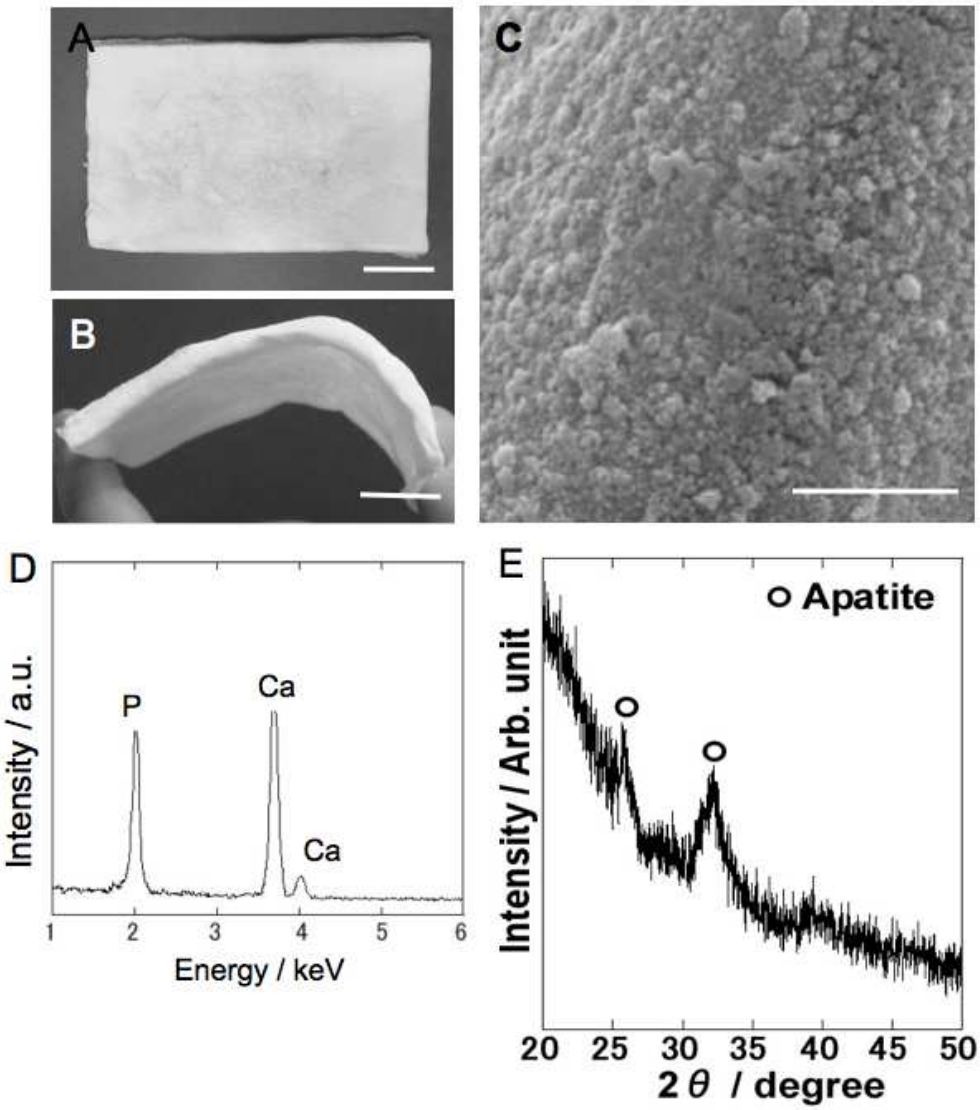

Apatite-coated hyaluronan (ACH) and its surface texture and property. (A) Overhead view of large-size ACH. Demonstration of ACH flexibility (B). SEM images (C), EDX data (D), and TF-XRD patterns (E) of the surface of ACH, which were formed through cross-linking with divinylsulfone, freeze-dried, washed with 1M CaCl2 for 24 h , and finally soaked in SBF for 7 days. Bar = 1.0 cm (A, B), 5 μm (C).
213x241mm (72 x 72 DPI)

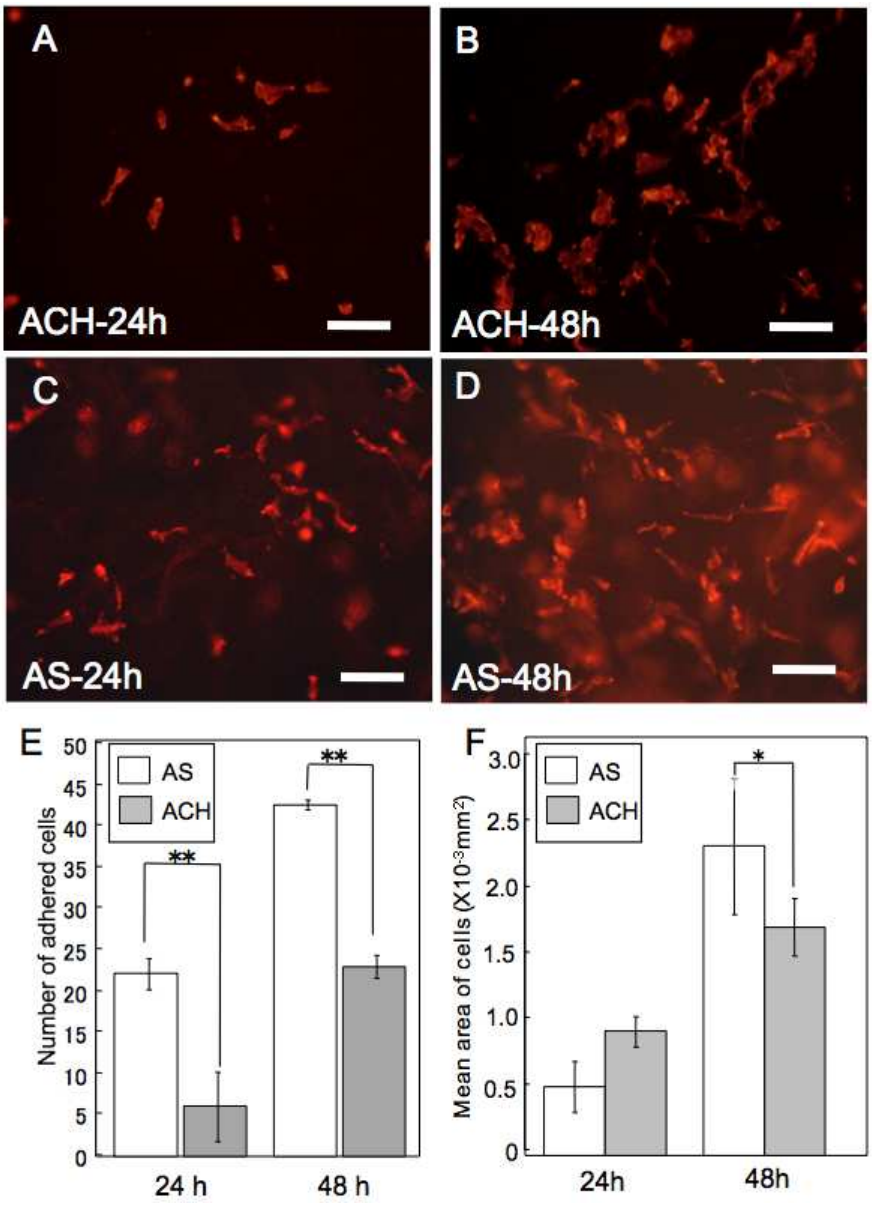

Attachment and spreading of osteoblastic cells cultured on ACH and atelocollagen sponge (AS). Fluorescent images showing actin fibers in osteoblastic cells cultured on apatite coated hyaluronan and atelocollagen sponge for 24 h and 48 h (A–D). Number (E) and mean area (F) of cells adhered to ACH and AS. Cells in 10 randomly selected fields (50 x 70 μm) were examined using a fluorescence microscope (Olympus Optical, Tokyo, Japan). Data represent mean ± SD. * $p < 0.05$, ** $p < 0.01$. Bar = 10 μm (A-D).
207x281mm (72 x 72 DPI)

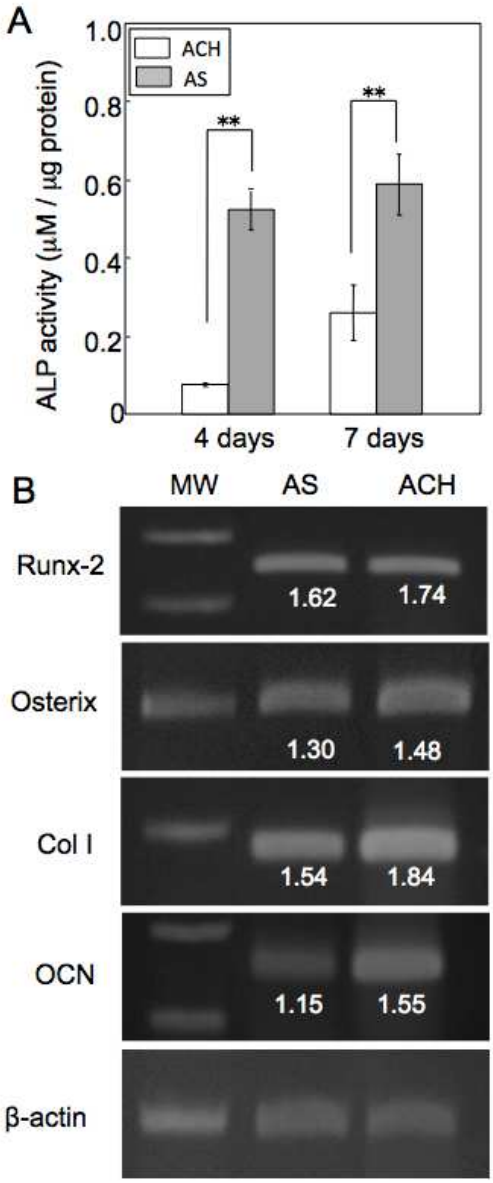

Alkaline phosphate activity and gene expression of the MC3T3-E1 cells on ACH and AS. (A) ALP activity of the 4 or 7days cultured MC3T3-E1 cells was monitored spectrophotometrically using a microplate reader (Model 55C; Bio-Rad, Tokyo, Japan). Sample protein concentrations were measured using a commercially available kit (Protein Assay Rapid Kit; Wako). Bovine serum albumin was used as a standard. Data represent mean ± SD. **$p < 0.01$. (B) Semi-quantitative RT-PCR analysis of the gene expression in the MC3T3-E1 cells on ACH and AS cultured for 14 days. Osteoblast differentiation markers, runx-2, osterix, type I collagen (Col I), and osteocalcin (OCN) were detected in cells grown on ACH and AS. Reproducibility of the RT-PCR data was confirmed by three or more replicate experiments. Data were analyzed using NIH Image software (NIH, Bethesda, MD, USA). Values represent levels of target mRNA expression, quantified relative to loading control (β-actin) signals. MW: molecular weight markers.
129x279mm (72 x 72 DPI)

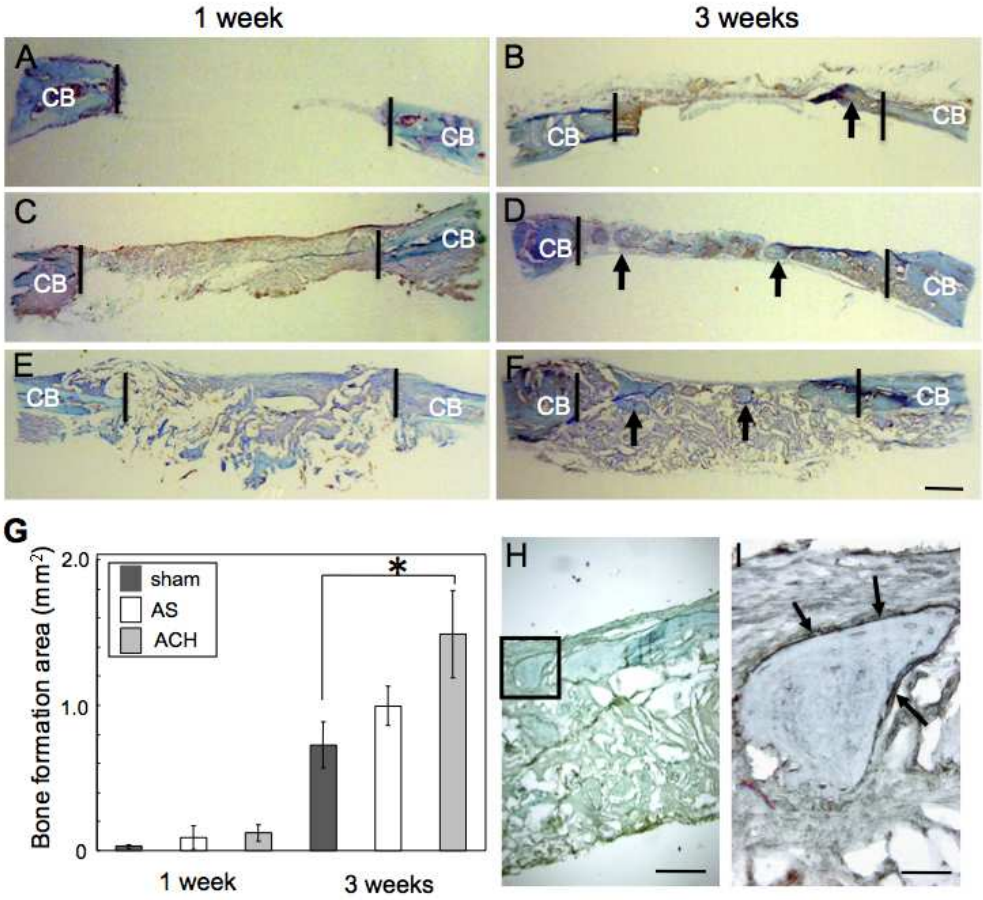

Bone regenerative properties of apatite-coated hyaluronan. Histological images show bone formation in sham (A, B), AS (C, D), and ACH-treated rats (E, F), 1 and 3 weeks after cranial bone defects were filled. CB: cranial bone. Vertical bars indicate the margins of the created bone defects. Arrows indicate newly formed bone. (G) Quantified areas of newly formed bone. Data represent means ± SD. *p < 0.05. (H) Immunohistochemical detection of osteopontin (OPN) on the apatite-coated hyaluronan group 3 weeks after surgery. (I) Higher magnification image of the highlighted region in (H). Arrows identify a layer of OPN-positive cells. All slides were counterstained with toluidine blue. Bar = 1 mm (A-F), 0.5 mm (H), and 0.1 mm (I).
259x239mm (72 x 72 DPI)